

THE FORMATION OF  $^{26}\text{Al}$  IN NOVA EXPLOSIONS

IRIT NOFAR AND GIORA SHAVIV

Department of Physics and Space Research Institute, Israel Institute of Technology, The Technion, Haifa, 32000 Israel

AND

SUMNER STARRFIELD<sup>1</sup>

Department of Physics and Astronomy 1504, Arizona State University, Tempe, AZ 85287-1504

Received 1990 May 14; accepted 1990 August 24

## ABSTRACT

The amount of  $^{26}\text{Al}$  in the interstellar medium, which has been detected both by the *HEAO 3*  $\gamma$ -ray spectrometer and the *SMM* experiment, in combination with the measured overabundance of  $^{26}\text{Mg}$  in meteorites, is predicted to have been produced by nucleosynthesis in nova explosions. To test this prediction, we have investigated the nucleosynthesis of  $^{26}\text{Al}$  during hot hydrogen burning along temperature-density-time profiles obtained from hydrodynamic simulations of nova outbursts. We find that we can predict the yield of  $^{26}\text{Al}$  if we characterize the thermonuclear runaway by means of two parameters: (1) the peak temperature and (2) the time required by the nova to reach peak temperature. We provide yields of  $^{26}\text{Al}$  in terms of these parameters. We have also found that the yield of  $^{26}\text{Al}$  is directly proportional to the abundances of the heavy elements so that about 20% of the initial  $^{24}\text{Mg}$  is converted into  $^{26}\text{Al}$ . Therefore, we are also able to show that the dominant contributor of  $^{26}\text{Al}$  to the Galaxy must be novae which occur on oxygen-neon-magnesium white dwarfs. However, we also find that the class of novae that should be the most important contributors to Galactic nucleosynthesis of  $^{26}\text{Al}$  may not have been discovered but must exist.

*Subject headings:* nucleosynthesis — stars: novae

## 1. INTRODUCTION

Although it was Urey (1955) who first suggested the importance of the radioactive decay of  $^{26}\text{Al}$  to the heating of the small bodies in the solar system, it was Lee, Papanastassiou, & Wasserburg (1977) who demonstrated that large excesses of  $^{26}\text{Mg}$  were correlated with the ratio of  $^{27}\text{Al}/^{24}\text{Mg}$  in the Allende meteorite. These authors concluded that  $^{26}\text{Al}$ , which is the radioactive parent of  $^{26}\text{Mg}$ , was present in the early solar system. Because of its short half-life,  $7.2 \times 10^5$  yr, this result also implied that it must have been produced by some astrophysical process shortly before the formation of the solar system and then mixed with the pre-solar nebula just prior to its collapse.

Its presence in the interstellar medium (ISM) was confirmed by the discovery, by *HEAO 3*, of 1.809 Mev  $\gamma$ -ray line emission which results from the decay of  $^{26}\text{Al}$  to the first excited state of  $^{26}\text{Mg}$  (Mahoney et al. 1982). Mahoney et al. also found that the  $\gamma$ -ray photons appeared to originate from the general direction of the Galactic plane. The Mahoney et al. (1982) result was later confirmed by measurements with the *SMM*  $\gamma$ -ray spectrometer (Share et al. 1985). Based on these results, Clayton (1984) concluded that the ISM contains about  $4.2 M_{\odot}$  of  $^{26}\text{Al}$ . The confirmation of the existence of  $^{26}\text{Al}$ , both in meteorites and the ISM, stimulated a variety of calculations to determine the astrophysical site and mechanisms that could produce this isotope. In the late 1970s it was realized that the most likely source was hot hydrogen burning (see Arnould et al. 1980; Clayton & Leising 1987). An excellent review of the  $^{26}\text{Al}$  problem can be found in Clayton & Leising (1987) and we refer the reader to that reference for more details.

In the next section we briefly report on the previous theoretical work that has been done to identify the site of  $^{26}\text{Al}$  production in the Galaxy. In § 3 we present the nova model that

served both as the basis of the temperature-density-time profiles used in our study and, in addition, provided some of the other initial parameters that were used in this work. In § 4 we discuss our procedures for searching parameter space in order to determine the maximum yield of  $^{26}\text{Al}$  from novae. In § 5 we report the results of our calculations and end, in § 6, with the conclusions and a discussion.

2. PRODUCTION OF  $^{26}\text{Al}$ 

The isotope  $^{26}\text{Al}$  is characterized by its short half-life,  $\tau = 7.2 \times 10^5$  yr, after which it decays into  $^{26}\text{Mg}$ . It is now thought that  $^{26}\text{Al}$  is produced by proton captures on  $^{25}\text{Mg}$  and that the magnesium is made in previous stellar generations. Ward & Fowler (1980) argued that  $^{26}\text{Al}$  cannot be synthesized at too high a temperature since both  $^{26g}\text{Al}$  and  $^{26m}\text{Al}$  (the “g” and “m” in the superscripts refer to the two isomeric states of  $^{26}\text{Al}$ ) are rapidly equilibrated and destruction occurs via  $(p, \gamma)$ ,  $(p, n)$ , and  $(n, \gamma)$  reactions at  $T_9 \approx 1.0$ – $2.0$ . Since the  $^{26}\text{Mg}$  anomaly in meteorites is not correlated with anomalous abundances of heavier nuclei, it seems likely that the production of  $^{26}\text{Al}$  can take place at temperatures as low as  $T_9 \leq 0.4$  (see also Champagne et al. 1983).

A possible mechanism for  $^{26}\text{Al}$  production is explosive hydrogen burning in the outer layers of a supernova (Arnould et al. 1980; Ward & Fowler 1980). Arnould et al. used a presupernova model of Weaver, Zimmermann, & Woosley (1978), for a  $25 M_{\odot}$  star, and calculated the ratio of  $^{26}\text{Al}/^{27}\text{Al}$  that would be expected from a supernova shock passing through the star. They found that negligible production of  $^{26}\text{Al}$  occurs in the inner zones since the proton concentration,  $X_p$ , is very low. They also found a low yield of  $^{26}\text{Al}$  in the outer layers because the temperatures were too low. Therefore, the most favorable location in the star for  $^{26}\text{Al}$  production was an intermediate region having both a mass of  $\sim 1.47 \times 10^{-2} M_{\odot}$  and a peak temperature in the shock of  $T_9 = 0.178$ . The peak ratio of

<sup>1</sup> Also Theoretical Division, Los Alamos National Laboratory.

$^{26}\text{Al}/^{27}\text{Al}$  found in their models was  $5 \times 10^{-2}$ . When post-explosion mixing of the various zones was included in their calculations, the average value of the ratio  $^{26}\text{Al}/^{27}\text{Al}$  was  $\sim 0.01$ . The value of  $^{26}\text{Al}/^{27}\text{Al}$  rose to  $\sim 1.0$  in an envelope with a mass of  $\sim 0.13 M_{\odot}$ .

Arnould et al. (1980) repeated these calculations for a  $15 M_{\odot}$  star and found insufficient production of  $^{26}\text{Al}$  because the temperatures and densities were too low throughout the star. Their results implied that only very massive stars might be able to eject a significant amount of  $^{26}\text{Al}$  in supernova explosions, and even there it was produced only in a narrow region within the interior of the presupernova star.

The idea that  $^{26}\text{Al}$  could be synthesized in the hot hydrogen burning that occurs during a nova explosion was proposed by Clayton & Hoyle (1974, 1976), Clayton (1984), and Arnould et al. (1980). In this mechanism, accretion of hydrogen-rich material onto a white dwarf produces a thermonuclear runaway (hereafter; TNR) in the degenerate accreted envelope of the white dwarf. The peak temperatures found in the simulations of the nova outburst (Starrfield 1989) are high enough ( $T > 2.0 \times 10^8$  K) so that one expects MgAl burning to produce sufficient yields of  $^{26}\text{Al}$  (Ward & Fowler 1980).

Preliminary studies by Chance & Harris (1979) and Arnould & Norgaard (1978) showed that production of  $^{26}\text{Al}$  could occur in the explosion of a  $^{14}\text{N}$ -rich layer. But the  $^{22}\text{Ne}$  mass fraction in the pre-explosion envelope had to be  $\sim 10^{-4}$  (Arnould & Norgaard 1978). However, this type of nucleosynthesis demanded a high temperature in the nuclear burning region:  $T_{\text{peak}} \approx 6 \times 10^8$ , which was much too high to produce large overabundances of  $^{26}\text{Al}$  (Ward & Fowler 1980).

Arnould et al. (1980), using the results of a hydrodynamic nova simulation computed by Starrfield, Truran, & Sparks (1978), found both the ratio of  $^{26}\text{Al}/^{27}\text{Al}$  varying from  $\approx 1.0$ – $1.8$ , and, in addition, that the ratio  $^{27}\text{Al}/^{27}\text{Al}_{\odot}$  was  $\approx 3.3$ . The amount of  $^{26}\text{Al}$  produced, per star, in the calculations reported by Arnould et al. (1980) was much higher than the amounts obtained in the attempts using supernova shocks but it was still not high enough to explain the observed overabundances of  $^{26}\text{Al}$ . Hillebrandt & Thielemann (1982) in a study which was also based on the models of Starrfield, Truran, & Sparks (1978) redid the calculations of Clayton & Hoyle (1976) and Vangioni-Flam, Audouze, & Chieze (1980), with an updated reaction network and different initial compositions. Their results for the ratio of  $^{26}\text{Al}/^{27}\text{Al}$  ranged from 0.66 to 1.34 in a set of calculations in which the model parameters were varied over the values  $0.146 \leq T_{9,\text{peak}} \leq 0.325$  and  $6.3 \times 10^3 \leq \rho_{\text{initial}} \leq 1.4 \times 10^4$  g cm $^{-3}$ . Finally, Wiescher et al. (1986) repeated the calculations of Hillebrandt & Thielemann (1982) using updated nuclear reaction rates but solar or carbon-oxygen initial compositions. They found that the yield of  $^{26}\text{Al}$  from nova explosions was small.

Based on these results, Clayton & Leising (1987) stated that ejecta from novae could “only explain the observed  $\gamma$ -ray emission when all the uncertainties in their production are pushed to the most optimistic limits.” We emphasize, however, that Wiescher et al. (1986) ignored any effects of mixing of the burning zone with the rest of the envelope (as do we) and also stated that varying the initial amount of Ne, Na, or Mg would change their results by only a factor of 3 to 5. However, we shall show that this is not the case and, if we assume as large an enhancement as is observed in novae ejecta (Starrfield 1988), the final isotopic ratios for these nuclei will change by large amounts.

Since the time that most of the earlier studies reported in this section were done, an important change in the problem of finding the source of  $^{26}\text{Al}$  has been the discovery of a class of novae with ejecta strongly enhanced in oxygen, neon, magnesium, and aluminum (Starrfield 1988). There are now at least four novae, that have been well-studied both in the optical and the ultraviolet, which are members of this class. In addition, another such nova has now been found in the LMC (LMC 1990 No. 1; Sonneborn, Shore, & Starrfield 1990, in preparation). Given the existence of this class of novae, one can assume that large amounts of oxygen, neon, and magnesium can be mixed from the core into the accreted envelope and that a significant fraction of the  $^{24}\text{Mg}$  can be transformed into  $^{26}\text{Al}$  by the TNR. We note that the calculations of Wiescher et al. (1986) did not include the type of abundance enhancements that one would expect from accretion and mixing onto an ONeMg white dwarf.

While it seems likely that  $^{26}\text{Al}$  can be formed at the peak temperatures which occur during a TNR on a white dwarf and which reproduce the observed features of a nova outburst, the production of  $^{26}\text{Al}$  still needs to be verified by calculations. Therefore, the main goals of this paper are the following: (1) to verify that TNRs in the accreted hydrogen-rich envelopes of white dwarfs do produce  $^{26}\text{Al}$ ; (2) to determine the temperatures and evolutionary time scales under which  $^{26}\text{Al}$  will be synthesized in a nova outburst; (3) to try to determine if there are observations of novae that can identify the novae that are producing  $^{26}\text{Al}$ , which is very important for studies of Galactic nucleosynthesis; and (4) to show that the observed abundances in ONeMg novae are characteristic of core material from an ONeMg white dwarf that has been mixed up into the accreted envelope, processed through hot hydrogen burning during the TNR, and then ejected into space.

### 3. THE NOVA MODEL

Starrfield, Sparks, & Shaviv (1988), in a study designed to simulate the outburst of the recurrent nova, U Sco, investigated the evolution of a  $1.35 M_{\odot}$  white dwarf that was accreting material at a high rate of mass accretion  $\sim 1.1 \times 10^{-6} M_{\odot}$  yr $^{-1}$ . Such a high rate was chosen to reproduce the observed short recurrence time of U Sco (8 yr). In their paper they found that, at that rate of accretion, it takes the white dwarf only 2.6 yr to reach a runaway and eject  $4 \times 10^{-7} M_{\odot}$ . Such a high rate of accretion is possible only if the secondary is a giant. They assumed that the accreted material had a large excess of He, 78%, because the observed helium abundance in U Sco is very high. We decided to use this model in our ONeMg nova study since it would be easier to produce heavier nuclei with such a He excess. The assumed abundances were  $X = 0.2$ ,  $Y = 0.78$  and the distribution in  $Z$  was divided according to the Suess-Urey semi-empirical solar abundance distribution (the abundances were obtained from the Landolt-Bornstein Tables; editor-in-chief K. H. Hellwege). However, other initial compositions were also used. The nuclear reaction network used in our work contained nuclei from hydrogen to phosphorus. The reaction rates were compiled from Fowler, Caughlan, & Zimmerman (1975), Harris et al. (1983), Wallace & Woosley (1981), Wagoner, Fowler, & Hoyle (1967), Nomoto et al. (1985), Wiescher et al. (1987), Arnould et al. (1980), and Thielemann (1989, private communication).

All our calculations are based on a tabulation of the variation of temperature and density with time in the deepest hydrogen-rich zone (a temperature-density-time profile)

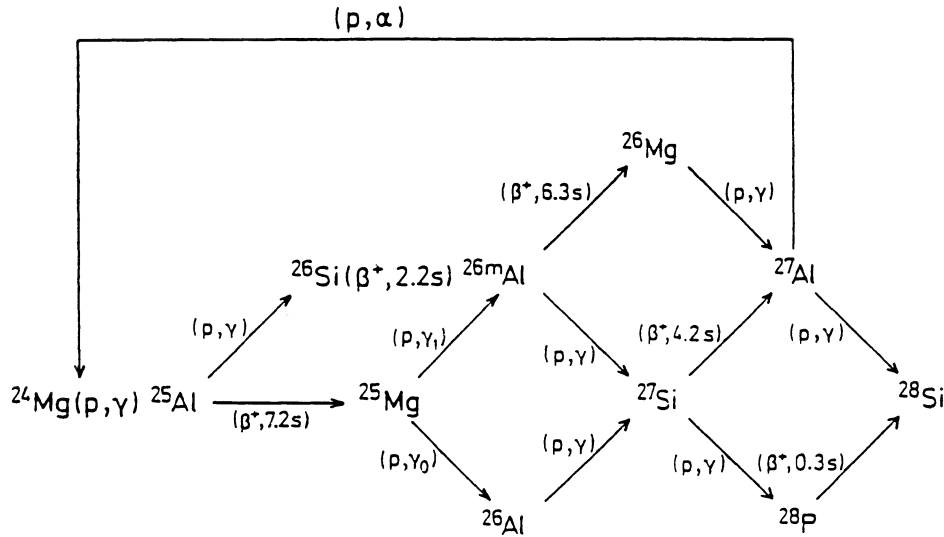


FIG. 1.—Most important reactions in the synthesis of  $^{26}\text{Al}$  (Arnould et al. 1980)

obtained from the nova simulations of Starrfield et al. (1988; Model 4 in their paper and shown in our Fig. 2). However, they stopped their calculations when the temperatures in the simulation were still high ( $T_g \approx 0.1$ ) and nuclear burning was still occurring at the bottom of the envelope. Therefore, we extrapolated their nuclear evolution by assuming that the layers are expanding adiabatically with  $\gamma = 5/3$  and only stopped the calculations when the temperatures had fallen to  $T_g = 0.01$ . This procedure does not change any of our results and only verifies that all significant nuclear burning has ended by the time that the temperatures have fallen to this value.

#### 4. METHODS

If we ignore the effects of composition, then the hydrodynamic simulations have shown that the characteristics of the

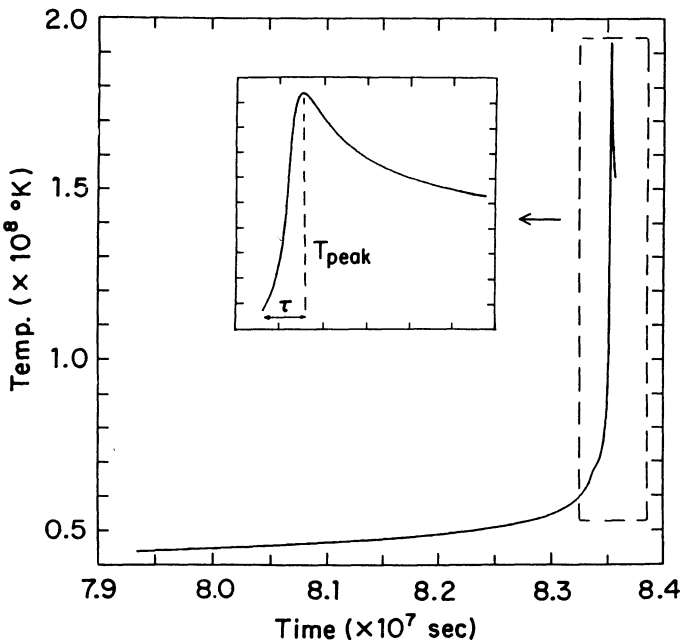


FIG. 2.—Temperature as function of time and the definitions of  $T_{\text{peak}}$  and  $\tau_{\text{ex}}$

nova outburst are sensitive to three parameters: (1) the mass of the white dwarf, (2) the luminosity of the white dwarf and, (3) the rate of mass accretion onto the surface of the white dwarf. As we shall show in the following sections, the amount of  $^{26}\text{Al}$  produced during the outburst is sensitive to only two parameters of the TNR, the peak temperature (hereafter,  $T_{\text{peak}}$ ) and the time that it takes the nuclear burning shell source to evolve from a temperature of  $10^8$  K to the peak temperature (hereafter;  $\tau_{\text{ex}}$ ). The quantity  $\tau_{\text{ex}}$  is shown in Fig. 2, but without the subscript “ex.” We chose  $T_{\text{peak}}$  and  $\tau_{\text{ex}}$  as the parameters to vary because many of the features of the outburst are correlated with these parameters. The density in the burning zone is unimportant, since MacDonald (1983) has shown that virtually all the TNRs in accreted white dwarf envelopes occur at about the same pressure at the base of the envelope. Thus, one need not specify the density behavior.

However, it is also appropriate to point out that our one zone calculations ignore the effects of convection. The hydrodynamic simulations have shown that, during the evolution of the TNR, a convective region forms just above the shell source and gradually grows to include the entire accreted envelope. The effects of convection on the TNR are discussed in detail elsewhere (see, for example, Starrfield 1989). Here, we only note that convection will both mix the products of nuclear burning to the surface regions and, in addition, mix fresh unburned nuclei into the nuclear burning region on short time scales. This should increase the abundances of those nuclei that are burned on a short time scale over the values to be reported in this work. We are testing this prediction in a calculation that includes the large network in a hydrodynamic simulation (Nofar, Shaviv, & Starrfield 1990, in preparation; Politano et al. 1990, in preparation). We note that it is more efficient, with respect to computer CPU time, to do a one-zone parameter study and then use our best predictions from the one-zone investigations in a hydrodynamic large nuclear reaction network study that will consume large amounts of computer time.

Our fundamental problem, therefore, is to find the regions in the  $T_{\text{peak}}-\tau_{\text{ex}}$  plane for which significant  $^{26}\text{Al}$  nucleosynthesis occurs and then to identify the class of novae whose ejected abundances show that its nuclear burning region evolved with

those particular parameters. We must emphasize, however, that finding these conditions does not, necessarily, mean that there is an observed class of novae that fit those parameters.

To proceed, we use tabulated values of the evolution of temperature and density with time in the layer where the temperature reached its maximum value for the model, and we have referred to this as the temperature-density-time profile. The depth where the temperature reached its maximum value was usually the zone which marks the interface between the core and accreted material. The temperature-density-time profile that we have chosen as the basis of this study is shown in Figure 2 and it was obtained from a hydrodynamic calculation of Starrfield et al. (1988) done with a small nuclear reaction network.

In some of our studies, the initial composition contained no  $^{27}\text{Al}$  so that some values of the final isotopic ratios that we report,  $^{26}\text{Al}/^{27}\text{Al}$  for example, will be upper limits. However, at the temperatures relevant to this study,  $^{27}\text{Al}$  is neither burned nor created.  $^{27}\text{Al}$  was included in the calculations done with initial abundances different from solar.

We approach our goal in four steps. First, we change all of the tabulated temperatures by a constant factor. In this way, the value of  $T_{\text{peak}}$  and the plateau change simultaneously. "Plateau" is our name for the long-time, low-temperature phase of the evolution which occurs after  $T_{\text{peak}}$  on the declining part of the evolution of the TNR. The purpose of this part of the study is to verify that the plateau has no effect on  $^{26}\text{Al}$  production. Second, we vary the value of  $T_{\text{peak}}$  but leave the temperatures of the plateau unchanged. Third, we change the value of  $\tau_{\text{ex}}$ . Fourth, we change the initial composition. This procedure was the most efficient way to find the values of  $T_{\text{peak}}$  and  $\tau_{\text{ex}}$  which, when used in our calculations, produced the maximum amount of  $^{26}\text{Al}$ .

## 5. NUMERICAL RESULTS

### 5.1. Changing the Temperature Profile by a Constant Factor

In the first part of our work we used the profile shown in Figure 2. We then investigated the sensitivity of  $^{26}\text{Al}$  production to an increase in all the temperatures in the profile as shown in Figure 3. The inset is an enlarged view of the region around  $T_{\text{peak}}$ . Here we were trying to determine the amount of  $^{26}\text{Al}$  that would be synthesized during the plateau, since all the numerical simulations show that the duration of this phase can vary tremendously from one TNR to another.

The results for the isotopic abundances from the reaction network are summarized in Table 1 and Figure 4, where the final abundance ratios of  $^{25}\text{Mg}/^{24}\text{Mg}$ ,  $^{26}\text{Mg}/^{24}\text{Mg}$  and  $^{26}\text{Al}/^{27}\text{Al}$  are shown as a function of  $T_{\text{peak}}$ . Note, that a very high ratio of  $^{26}\text{Al}/^{27}\text{Al}$  is found for  $T_0 \ll 0.13$ . As  $T_{\text{peak}}$  decreases, the  $^{26}\text{Al}/^{27}\text{Al}$  ratio increases but the total yield of  $^{26}\text{Al}$  decreases (see Fig. 4a). This increase is caused because, at these low temperatures, we neither produce nor burn  $^{27}\text{Al}$ . For some cases the isotopic ratio can reach values as large as 100 but by that time the yield of  $^{26}\text{Al}$  is so low that it can be ignored.  $^{26}\text{Al}$  is not produced until  $T_0$  reaches  $\approx 0.09$  and the time it takes for the TNR to evolve to this temperature is unimportant for the production of  $^{26}\text{Al}$ . Therefore, the most important factor in producing a large amount of  $^{26}\text{Al}$  is the evolution time that the TNR spends near peak temperature not the long evolution time that it spends accreting the hydrogen-rich envelope.

At temperatures  $T_0 \geq 0.13$ , the mass fraction of  $^{26}\text{Al}$  increases to a value of  $\sim 10^{-5}$ . Model 3 produces the highest

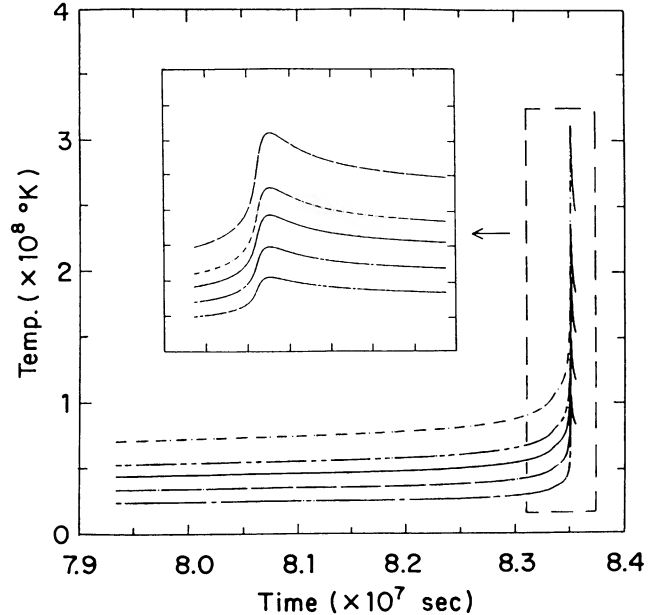


FIG. 3.—Temperature profiles used in the calculations described in Section V-A.

isotopic ratio of  $^{26}\text{Al}/^{27}\text{Al}$ ,  $\sim 21$ , while  $^{27}\text{Al}/^{27}\text{Al}_\odot \approx 1$ . All the models with  $0.1 \leq T_{0,\text{peak}} \leq 0.19$  produced virtually the same ratio of  $^{26}\text{Al}/^{27}\text{Al}$  but the mass fraction of  $^{26}\text{Al}$  decreased slightly as  $T_{\text{peak}}$  was increased. There is a second maximum in the ratio of  $^{26}\text{Al}/^{27}\text{Al}$  at a peak temperature of  $T_0 = 0.3$ , but the value of the ratio is smaller than we found at lower temperatures. Because of the smaller yield of  $^{26}\text{Al}$ , this peak is less significant.

Figure 4c shows that the reduction in  $^{26}\text{Al}$ , at peak temperatures around  $T_0 = 0.2$ , is accompanied by an excess of  $^{26}\text{Mg}$ . As the temperature rises to values of  $T_0 = 0.3$ , the yield of  $^{26}\text{Al}$  increases and a large excess of  $^{25}\text{Mg}$  appears. Inspection of the reactions in the MgAl cycle (see Fig. 1) shows that when the temperature is low,  $^{25}\text{Mg}$  is produced through the decay of  $^{25}\text{Al}$ . Then, after the capture of a proton onto  $^{25}\text{Al}$ , the more likely nucleus to be produced, according to the reaction rates, is  $^{26}\text{Al}$ . Therefore, an excess of  $^{26}\text{Al}$  should correlate with an excess of  $^{25}\text{Mg}$  and a concomitant reduction in  $^{26}\text{Mg}$ .

As we increase the temperature, the  $\beta$  decay of  $^{25}\text{Al}$  competes with proton captures on the same element. If the tem-

TABLE 1  
ABUNDANCES OBTAINED FROM MODELS WITH VARIOUS PEAK TEMPERATURES

Element	Model 1	Model 2	Model 3	Model 4	Model 5
$T_{\text{max}}$ .....	1.05+8	1.48+8	1.93+8	2.32+8	3.1+8
$T_{\text{start}}$ .....	2.37+7	3.35+7	4.40+7	5.25+7	7.02+7
H .....	1.9-1	1.7-1	2.8-2	1.0-10	1.7-9
$^4\text{He}$ .....	7.8-1	8.1-1	9.5-1	9.8-1	9.8-1
$^{40}\text{Ne}$ .....	3.9-3	3.9-3	3.1-3	2.4-3	3.8-3
$^{21}\text{Ne}$ .....	5.9-8	5.6-6	4.4-8	1.6-7	4.0-7
$^{22}\text{Ne}$ .....	1.0-8	4.9-9	3.4-9	5.0-8	1.7-5
$^{22}\text{Na}$ .....	1.2-6	9.9-7	3.8-7	2.6-13	8.0-11
$^{23}\text{Na}$ .....	1.1-5	5.3-6	2.6-7	1.1-5	1.1-5
$^{24}\text{Mg}$ .....	1.4-4	2.5-6	1.0-6	1.0-6	2.5-6
$^{25}\text{Mg}$ .....	3.9-4	5.4-4	1.5-4	3.2-5	6.6-4
$^{26}\text{Mg}$ .....	9.4-8	4.5-5	1.1-3	1.7-3	7.2-6
$^{26}\text{Al}$ .....	3.2-8	5.1-5	3.2-5	1.5-5	3.3-6
$^{27}\text{Al}$ .....	5.6-10	2.8-6	1.5-6	3.4-6	4.2-7

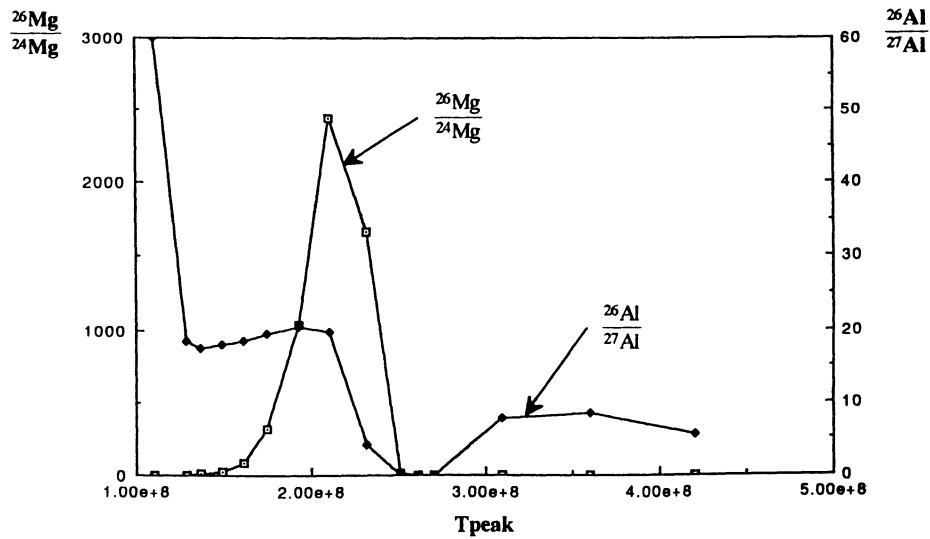
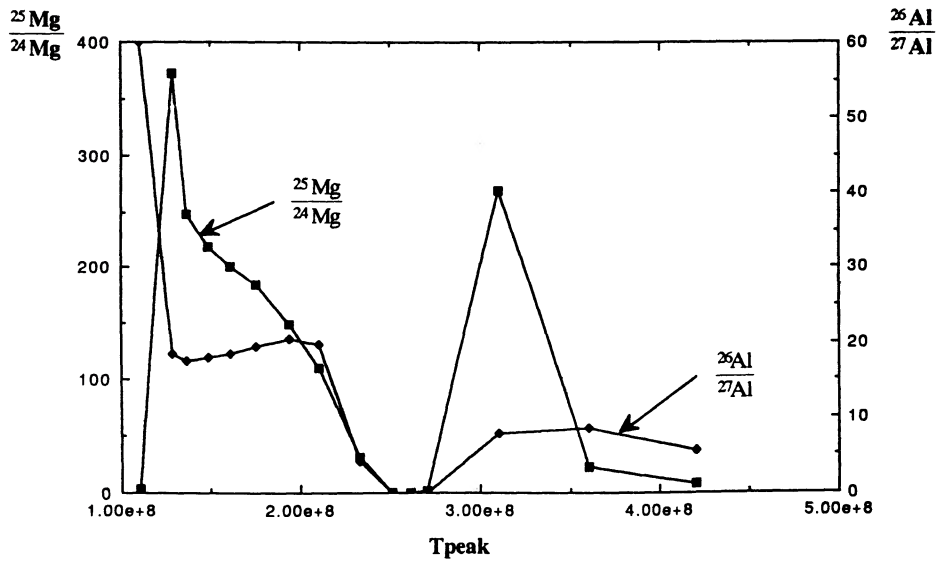
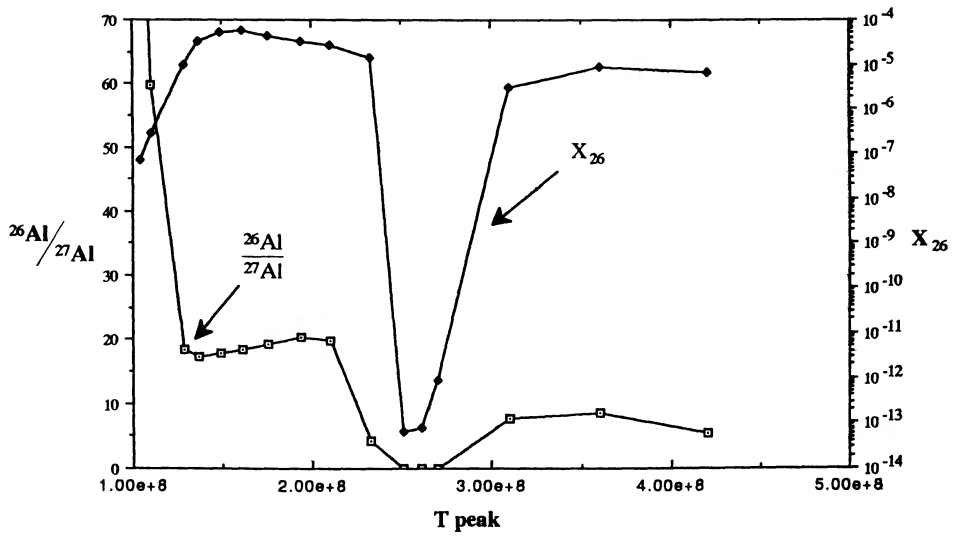


FIG. 4.—Final abundances and abundance ratios for selected nuclei as a function of the peak temperature (see § 5.1). (a) Abundance by mass of  $^{26}\text{Al}$  ( $X_{26}$ ) and the ratio of  $^{26}\text{Al}/^{27}\text{Al}$  as functions of  $T_{\text{peak}}$ . (b) Same as for Fig. 4a but for  $^{25}\text{Mg}/^{24}\text{Mg}$ . The ratio of  $^{26}\text{Al}/^{27}\text{Al}$  is shown for comparison. (c) Same as for Fig. 4a but for  $^{26}\text{Mg}/^{24}\text{Mg}$ . The ratio of  $^{26}\text{Al}/^{27}\text{Al}$  is shown for comparison.

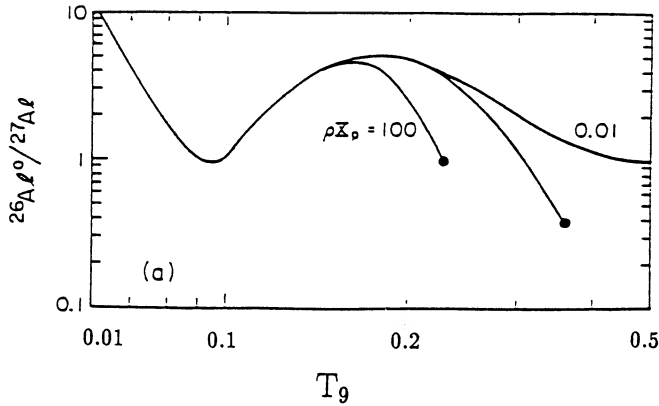


FIG. 5.—Temperature dependence of the steady-state abundance ratio of  $^{26}\text{Al}/^{27}\text{Al}$ . Taken from Ward & Fowler (1980).

perature is not too high,  $^{26}\text{Si}$  decays into  $^{26m}\text{Al}$  and then into  $^{26}\text{Mg}$ . Therefore, we expect the overabundance of  $^{26}\text{Mg}$  to be correlated with a reduction in the abundance of  $^{26}\text{Al}$ . If the temperature continues to increase, then  $^{26}\text{Si}$  can capture a proton ( $^{26}\text{Si}(p, \gamma)^{27}\text{P}$ ), which will probably decay into  $^{27}\text{Si}$ . However, since none of these reactions contribute to the synthesis of  $^{26}\text{Al}$ , the only way to produce  $^{26}\text{Al}$  is through the MgAl cycle.

Ward & Fowler (1980) presented a formal analytical framework for determining the means by which simple two- and three-level nuclei can attain a thermal distribution of excited-state populations in the stellar interior. They explored the case of  $^{26}\text{Al}$  both in the ground state and in the isomeric state and calculated the abundance ratio for a constant stellar temperature assuming that the MgAl cycle was in a steady state. Figure 5, taken from their paper, shows the temperature dependence of the steady state abundance ratio of  $^{26}\text{Al}/^{27}\text{Al}$ . The family of curves is given for the same value of  $\rho X_p$ . They predicted that the peak value for the ratio of  $^{26}\text{Al}/^{27}\text{Al}$  would occur near  $T_9 \approx 0.17$  and then would decrease as the temperature increased. Our results, which predict that the peak value of  $^{26}\text{Al}/^{27}\text{Al}$  occurs at  $T_9 \approx 0.19$ , are in excellent agreement with those of Ward & Fowler (1980). We note that, in terms of total mass fraction, the highest value of  $^{26}\text{Al}$  ( $\sim 6 \times 10^{-5}$ ) is found at  $T_{9, \text{peak}} = 0.17$ . This is the same temperature that both Ward & Fowler (1980) and Arnould et al. (1980) predicted would exhibit the highest ratio of  $^{26}\text{Al}/^{27}\text{Al}$ . For  $T_{9, \text{peak}} \ll 0.14$ , Ward & Fowler (1980) predicted (Fig. 5) a high ratio of  $^{26}\text{Al}/^{27}\text{Al}$  and, according to our calculations, the ratio is high but the mass fraction of  $^{26}\text{Al}$  is small.

### 5.2. Changing the Value of Peak Temperature

We proceed as if the TNRs in accreting white dwarfs evolve to maximum temperature along the same path, but then assume that they differ both in the value of  $T_{\text{peak}}$  and its duration. We are aware that this approach simplifies the evolution of the TNR, but our results show that the two most important parameters, for the resulting nucleosynthesis, are  $T_{\text{peak}}$  and  $\tau_{\text{ex}}$ . As was shown in the last subsection, the evolution time, when the temperature is below  $T_9 = 0.09$ , has no effect on the results. Thus, we do not change the characteristics of the evolution when the temperature is below  $T_9 = 0.09$ , but only tabulate the amount of  $^{26}\text{Al}$  that is produced as a function of the height of  $T_{\text{peak}}$ . The isotopic ratios which result from this set of models are summarized in Table 2 and Figure 6. We see that Model 2

TABLE 2

FINAL ABUNDANCES WHEN JUST PEAK TEMPERATURE IS CHANGED

Element	Model 1	Model 2	Model 3	Model 4	Model 5
$T_{\text{max}}$ .....	1.17+8	1.7+8	1.9+8	2.2+8	2.5+8
$T_{\text{start}}$ .....	4.4+7	4.4+7	4.4+7	4.4+7	4.4+7
H .....	1.9-1	1.1-1	2.8-2	3.9-5	4.6-12
$^4\text{He}$ .....	7.8-1	8.7-1	9.5-1	9.8-1	9.8-1
$^{20}\text{Ne}$ .....	3.9-3	3.7-3	3.1-3	2.0-3	1.2-3
$^{21}\text{Ne}$ .....	5.8-8	5.1-8	4.4-8	8.1-8	2.2-7
$^{22}\text{Ne}$ .....	1.1-8	8.1-9	3.4-9	4.3-9	2.9-8
$^{22}\text{Na}$ .....	1.3-6	7.6-7	3.8-7	5.8-8	1.5-14
$^{23}\text{Na}$ .....	1.1-5	4.3-6	2.6-7	5.4-7	4.6-6
$^{24}\text{Mg}$ .....	1.2-5	2.2-6	1.0-6	4.9-7	7.6-6
$^{25}\text{Mg}$ .....	5.3-4	4.3-4	1.5-4	4.1-5	1.1-5
$^{26}\text{Mg}$ .....	4.8-7	3.3-4	1.1-3	2.1-3	2.5-3
$^{26}\text{Al}$ .....	1.6-6	5.6-5	3.2-5	2.2-5	1.8-11
$^{27}\text{Al}$ .....	5.9-8	2.9-6	1.5-6	1.4-6	2.2-5

again produces the highest yield of  $^{26}\text{Al}$ . Our results also clearly indicate that as long as  $T_{\text{peak}}$  is below  $T_9 = 0.25$ , the total production of  $^{26}\text{Al}$  does not depend on the exact shape of the evolution in temperature.

On the other hand, once  $T_{\text{peak}}$  exceeds  $T_9 = 0.25$ , we start to see differences in the resulting nucleosynthesis (Figs. 4 and 6). In particular, if we raise the entire profile so that  $T_{\text{peak}}$  exceeds  $\sim T_9 = 0.32$ , then there is a second peak in the abundances of  $^{26}\text{Al}$  and  $^{25}\text{Mg}$  (Fig. 4). There was no evidence for these peaks when only  $T_{\text{peak}}$  was changed (Fig. 6). The reason for the formation of the second peak can be traced to the particular variation of temperature with time used in this evolution. The  $^{26}\text{Al}$ , which was formed during the second peak ( $T_9 \sim 0.3$ ), was created during the “low-temperature phase” (see Fig. 2).

The temperature-time profiles used in this section are more realistic representations of the hydrodynamic simulations than the profiles that were used in § 5.1. During the quiet phase of the evolution, when the white dwarf is accreting mass and most of the heat input is coming from compression, the temperature in the shell source is below  $\sim 6-7 \times 10^7$  K and  $^{26}\text{Al}$  is not produced. Once the temperature reaches  $\sim 7 \times 10^7$  K, the TNR rapidly evolves to peak temperature. The nova simulations have shown that the temperature at the peak depends on the mass of the white dwarf, the amount of mass which was accreted, the rate of accretion, the luminosity of the white dwarf, and the chemical composition. Given all these parameters,  $T_{\text{peak}}$  can vary from  $10^8$  K, for the lowest mass white dwarfs, to values exceeding  $\sim 3 \times 10^8$  K for the highest mass white dwarfs. In addition, the highest peak temperatures, for a white dwarf of a given mass, occur on the lowest luminosity white dwarfs with accretion onto the white dwarf at values below  $\sim 10^{-10} M_{\odot} \text{ yr}^{-1}$ .

Our results show that a TNR, with  $T_{\text{peak}} \sim 2.5 \times 10^8$  K and  $\tau_{\text{ex}}$  about  $10^4$  s, produces a large amount of  $^{26}\text{Al}$ . This is an encouraging result since it means that the nova simulations, which most closely resemble the observations, are the same simulations that produce large amounts of  $^{26}\text{Al}$ .

### 5.3. Changing $\tau_{\text{ex}}$

The second crucial parameter in this investigation is  $\tau_{\text{ex}}$ , which is the time required for the rapidly growing temperature in the shell source to reach  $T_{\text{peak}}$ . The third crucial parameter, which will be discussed in a later subsection, is the initial abundances of the intermediate mass elements. In this section we

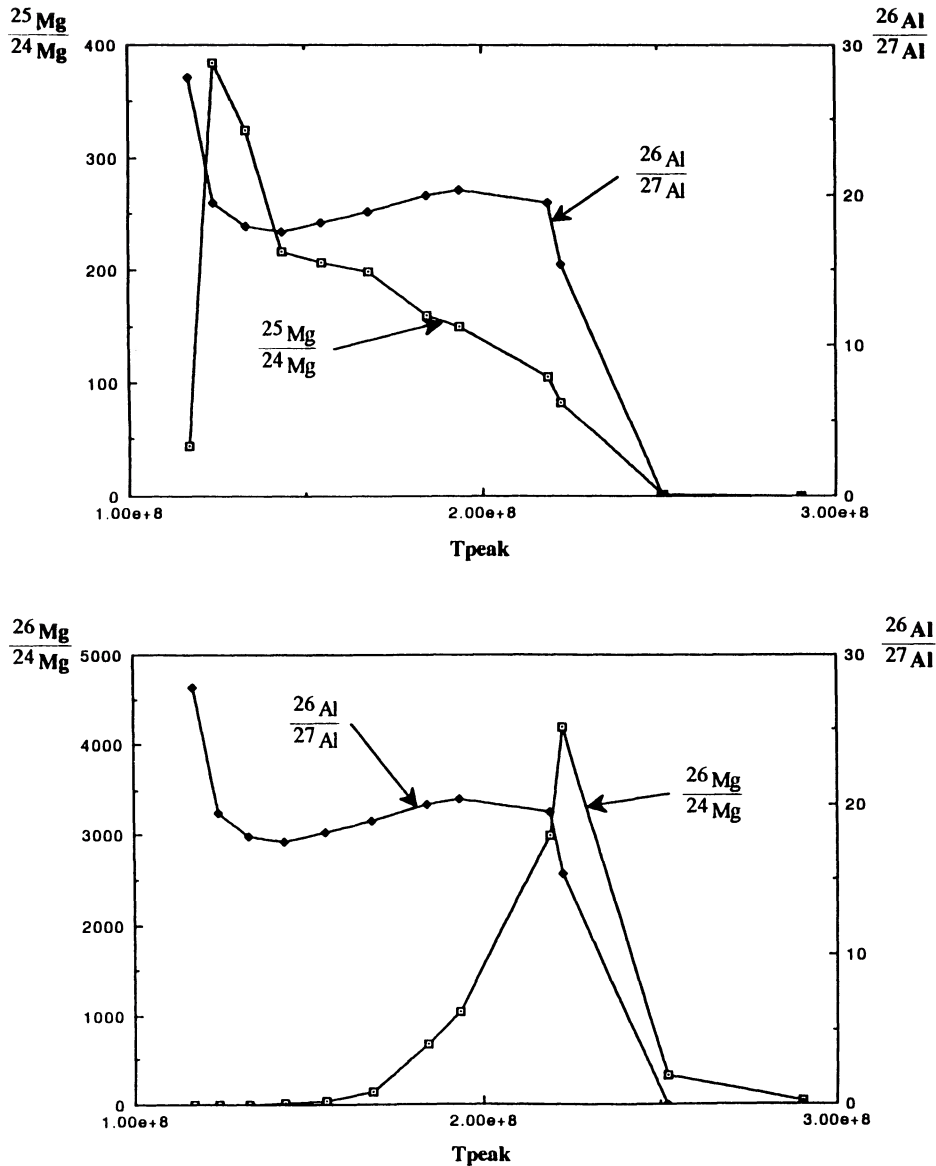


FIG. 6.—Final abundance ratios for selected nuclei as a function of peak temperature (§ 5.2). (b) Same as Fig. 6a but for different isotopic abundance ratios.

examine the effect of varying  $\tau_{\text{ex}}$  but holding  $T_{\text{peak}}$  constant. The time scale for the rise to peak temperature depends on the degree of electron degeneracy and the calculations of the outburst show that the more degenerate the material, the smaller the value of  $\tau_{\text{ex}}$ . The degree of degeneracy, when accretion begins, depends on the mass of the white dwarf. We, therefore, also carried out the calculations for several peak temperatures. Our results are summarized in a three-dimensional plot (Fig. 7) and in Table 4. In this figure we show, as a function of  $T_{\text{peak}}$  versus  $\tau_{\text{ex}}$ , either  $^{26}\text{Al}/^{27}\text{Al}$ ,  $^{25}\text{Mg}/^{24}\text{Mg}$ , or  $^{26}\text{Mg}/^{24}\text{Mg}$ . We normalized  $\tau_{\text{ex}}$  so that the value of  $\tau_{\text{ex},0}$ , which is  $1.1 \times 10^4$  s (see Fig. 2), is equal to 1. Table 4 tabulates the mass fractions of both  $^{26}\text{Al}$  and  $^{27}\text{Al}$  as a function of  $T_{\text{peak}}$  and  $\tau_{\text{ex}}$ .

We find that  $^{26}\text{Al}$  can be produced at temperatures as high as  $T_9 = 0.25$  provided that the value of  $\tau_{\text{ex}}$  lies between 100 and  $\sim 1000$  s, since evolution times that are this short prevent the destruction of  $^{26}\text{Al}$  that would normally occur at high tem-

peratures. We also decreased  $\tau_{\text{ex}}$  to values below  $\sim 10$  s, a value which is unrealistically short for a TNR in a white dwarf envelope. However, with such a small amount of time near  $T_{\text{peak}}$ , the yield of  $^{26}\text{Al}$  was too small to be significant for temperatures that exceed  $T_9 = 0.27$ .

#### 5.4. The Abundance of $^{26}\text{Al}$ in the $T_{\text{peak}}, \tau_{\text{ex}}$ Plane

The results are now presented as lines of equal (final)  $^{26}\text{Al}$  production in the  $T_{\text{peak}}$  versus  $\tau_{\text{ex}}$  plane (Fig. 8 and Table 4). This figure shows our main conclusion:  $^{26}\text{Al}$  is produced in significant amounts for only a small range of combinations of  $T_{\text{peak}}$  and  $\tau_{\text{ex}}$ . We also plot on this figure the values of  $T_{\text{peak}}$  and  $\tau_{\text{ex}}$  obtained in various hydrodynamic nova simulations. The white dwarf mass and mass accretion rate for each plotted point are given in the figure caption. The models for  $1.35 M_{\odot}$  are taken from Starrfield, Sparks, & Shaviv (1988) and were calculated using a variety of accretion rates and different

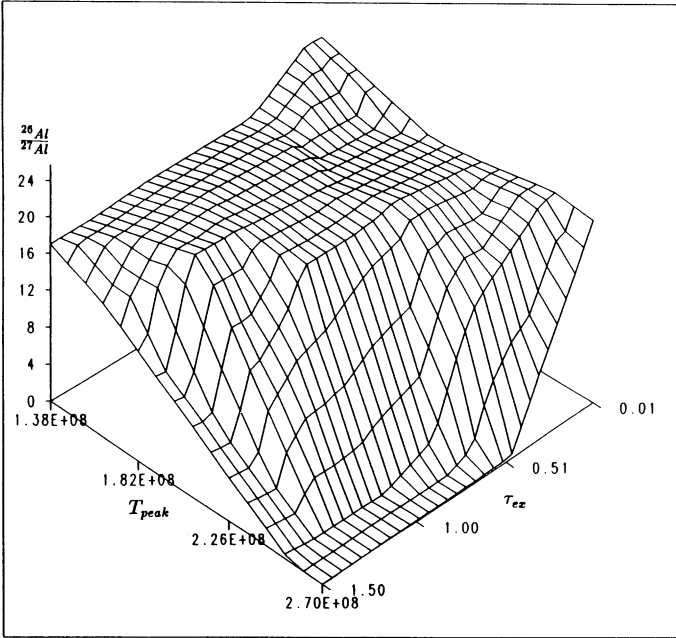


FIG. 7a

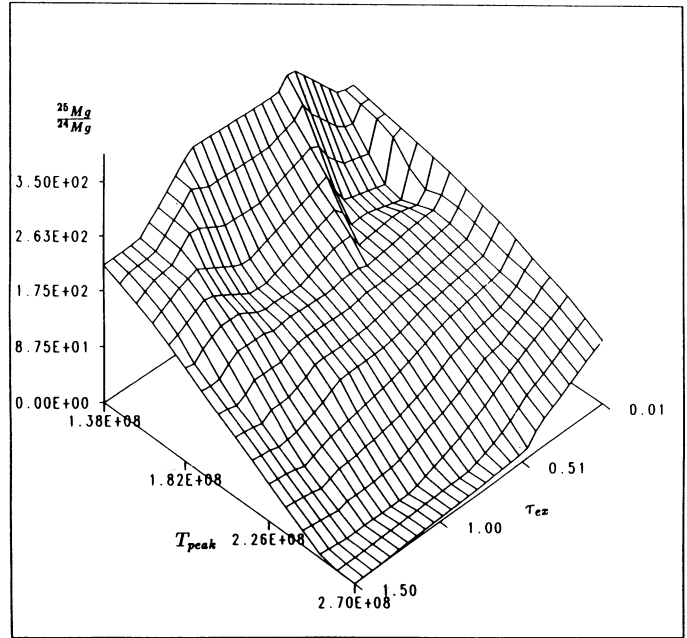


FIG. 7b

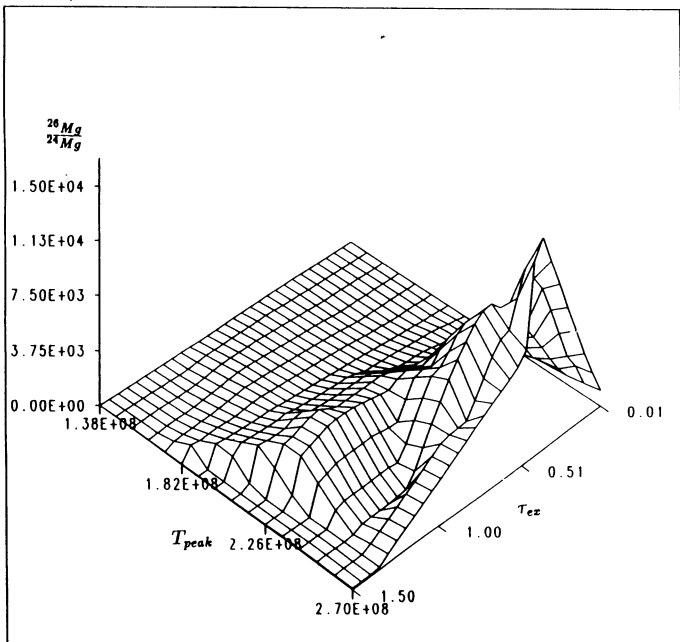


FIG. 7c

FIG. 7.—This plot shows the variation of the ratio of <sup>26</sup>Al/<sup>27</sup>Al as a function of  $T_{\text{peak}}$  and  $\tau_{\text{ex}}$ . (b) Same plot for <sup>26</sup>Mg/<sup>24</sup>Mg. (c) Same plot for <sup>26</sup>Mg/<sup>24</sup>Mg.

values for the fraction of the boundary layer accretion luminosity that is radiated into the star (called  $\alpha$  in their paper). That is,

$$L_{\text{acc}} = \alpha \frac{1}{2} \frac{GM}{R} \dot{M}.$$

The  $1.38 M_{\odot}$  model is taken from Starrfield, Sparks, & Truran (1985) (see Table 1 in their paper). Their first simulation

had an initial white dwarf luminosity of  $L/L_{\odot} = 0.1$ , a radius of  $R = 1.9 \times 10^8$  cm,  $T_e = 6.2 \times 10^4$  K, and the rate of accretion onto the surface was  $1.7 \times 10^{-8} M_{\odot} \text{ yr}^{-1}$ . For the second simulation, the parameters were  $L/L_{\odot} = 0.01$ ,  $R = 1.6 \times 10^9$  cm,  $T_e = 3.8 \times 10^4$ , and  $\dot{M} = 1.7 \times 10^{-9} M_{\odot} \text{ yr}^{-1}$ . The differences in the initial conditions for these two evolutionary sequences lead to different temperature histories and, consequently, to different yields of <sup>26</sup>Al. The values of  $T_{\text{peak}}$  and  $\tau_{\text{ex}}$ , obtained from these two calculations, suggest that they would be very inefficient at producing <sup>26</sup>Al. This implies that both the luminosity and mass accretion rate onto a white dwarf, of a given mass, will be important in determining if a given hydrodynamic simulation produces <sup>26</sup>Al. The  $1.25 M_{\odot}$  results were obtained from the calculations of accretion, at various rates, onto  $1.25 M_{\odot}$  white dwarfs done by Prialnik et al. (1982).

We note that different values of  $T_{\text{peak}}$  and  $\tau_{\text{ex}}$  are found when the nova simulations ignore accretion and begin with the envelope in place and in both hydrostatic and thermal equilibrium. Since this is not a good physical assumption, except when the accretion rates are low, we do not plot the results from such models in Figure 8. Furthermore, previous estimates of the total amount of <sup>26</sup>Al production in the galaxy (see

TABLE 3  
ELEMENT ABUNDANCES WHEN THE INITIAL Z IS CHANGED

Z	$T_{\text{peak}}$	<sup>26</sup> Al	<sup>27</sup> Al
20% .....	1.6+8	1.13-3	5.44-5
10% .....	1.6+8	3.36-4	1.72-5
2% .....	1.6+8	3.79-5	2.24-6
20% .....	1.8+8	1.53-3	9.52-5
10% .....	1.8+8	4.08-4	2.01-5
2% .....	1.8+8	3.35-5	1.68-6
20% .....	2.5+8	9.33-7	9.52-5
10% .....	2.5+8	5.97-12	8.31-5
2% .....	2.5+8	7.01-9	5.85-6



TABLE 4  
FINAL ELEMENTAL ABUNDANCES AS A  
FUNCTION OF  $T_{\text{peak}}$  AND  $\tau_{\text{ex}}$

$T_{\text{peak}}$	$\tau_{\text{ex}}^a$	$^{26}\text{Al}$	$^{27}\text{Al}$
2.7+8.....	1.0	1.3-14	2.2-4
	0.01	1.1-6	8.6-7
2.5+8.....	1.1	1.2-13	3.66-5
	1.0	1.7-11	2.23-5
	0.2	2.1-5	9.0-6
	0.1	2.4-5	1.16-6
	0.01	3.9-5	9.9-7
1.9+8.....	0.001	3.6-5	1.68-7
	1.1	3.2-5	1.55-6
	1.0	3.8-5	1.55-6
	0.2	3.8-5	2.01-6
	0.1	4.7-5	2.53-6
1.3+8.....	0.01	5.6-5	3.2-6
	0.001	5.1-6	2.7-6
	1.0	1.3-5	9.79-7
	0.2	9.1-6	6.8-7
	0.1	7.1-6	3.1-7
0.01	3.0-8	1.66-10	
0.001	4.3-8	2.9-10	

<sup>a</sup> Units:  $1.1 \times 10^4$  s.

Clayton & Leising 1987) were based on the assumed mass loss per event of  $\sim 10^{-4} M_{\odot}$ . This figure was obtained for nova calculations done on low-mass white dwarfs, and it is probably too high. A better estimate, for the maximum mass ejected in a single nova eruption, is  $\sim 10^{-5} M_{\odot}$ , which imposes a strong constraint on the galactic nucleosynthesis of  $^{26}\text{Al}$  by novae.

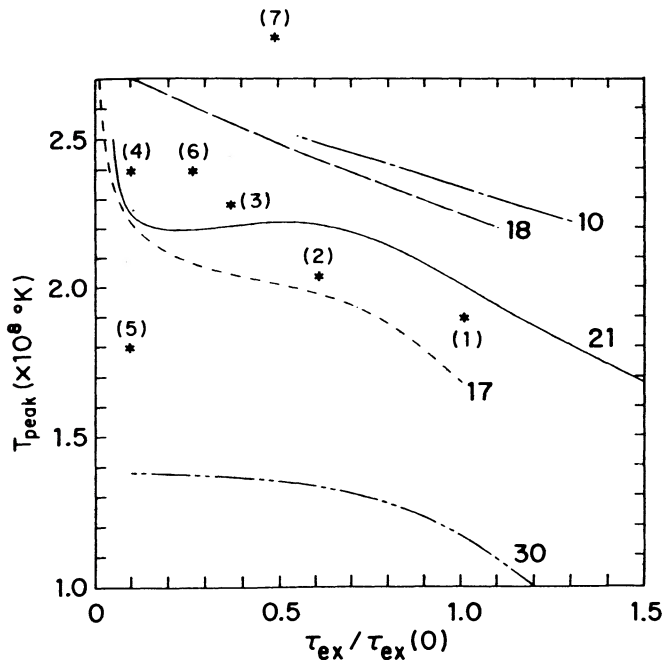


FIG. 8.—Lines of constant  $^{26}\text{Al}/^{27}\text{Al}$  in the  $T_{\text{peak}}, \tau_{\text{ex}}$  plane. The numbers near the lines are the values of  $^{26}\text{Al}/^{27}\text{Al}$ . The numbers in parentheses next to asterisks are the results from various nova models (see text). The details are the following: (1\*)  $1.35 M_{\odot}$ ,  $\dot{M} = 1.1 \times 10^{-6} M_{\odot} \text{ yr}^{-1}$ . (2\*)  $1.35 M_{\odot}$ ,  $\dot{M} = 1.6 \times 10^{-7} M_{\odot} \text{ yr}^{-1}$ . (3\*)  $1.35 M_{\odot}$ ,  $\dot{M} = 1.6 \times 10^{-8} M_{\odot} \text{ yr}^{-1}$ . (4\*)  $1.25 M_{\odot}$ ,  $\dot{M} = 10^{-10} M_{\odot} \text{ yr}^{-1}$ . (5\*)  $1.25 M_{\odot}$ ,  $\dot{M} = 10^{-8} M_{\odot} \text{ yr}^{-1}$ . (6\*)  $1.38 M_{\odot}$ ,  $\dot{M} = 1.7 \times 10^{-8} M_{\odot} \text{ yr}^{-1}$ . (7\*)  $1.38 M_{\odot}$ ,  $\dot{M} = 1.7 \times 10^{-9} M_{\odot} \text{ yr}^{-1}$ .

### 5.5. Changing $Z$

We also checked the sensitivity of our results to the abundances of the heavy elements by varying the initial composition. Our results for this series of calculations are summarized in Table 3 and Figure 9. These results clearly indicate that the mass fraction of  $^{26}\text{Al}$  is proportional to  $Z$  in the sense that the higher the value of  $Z$ , the larger the amount of  $^{26}\text{Al}$  produced by our calculation. We also find that the ratio of  $^{26}\text{Al}/^{27}\text{Al}$  can become extremely large as we vary the value of  $T_{\text{peak}}$ . For example, we chose an initial value of  $Z = 20\%$  and an initial abundance for  $^{27}\text{Al}$  of  $3.89 \times 10^{-5}$ . At the end of the calculations with  $T_{\text{peak}} = 2.2 \times 10^8$  K, the abundance (by mass) of  $^{26}\text{Al}$  was  $4.4 \times 10^{-4}$  and that of  $^{27}\text{Al}$  was  $3.2 \times 10^{-5}$ . However, when we reduced the value of  $T_{\text{peak}}$  to  $1.7 \times 10^8$  K, we found that the abundance of  $^{26}\text{Al}$  had increased to  $1.7 \times 10^{-3}$  while the abundance of  $^{27}\text{Al}$  had decreased to  $5 \times 10^{-9}$ . This result implies that the ONeMg novae that we are observing are probably ejecting mostly  $^{26}\text{Al}$ . We performed several calculations with overabundances of O, Ne, and Mg ( $X_{\text{O}} + X_{\text{Ne}} + X_{\text{Mg}} \leq 30\%$  of the initial composition), and we find that the mass fraction of  $^{26}\text{Al}$  in the ejected material can reach 5%. However, no matter what values were chosen for the initial composition ( $Z$ ), if the peak temperature in the calculation exceeded  $T_p = 0.27$ , then there was no significant yield of  $^{26}\text{Al}$ .

### 6. SUMMARY AND CONCLUSIONS

As a result of the calculations reported in this paper, we have found that it is possible to make significant amounts of  $^{26}\text{Al}$  during the thermonuclear runaway that is commonly assumed to be the cause of the nova outburst. However, the material in which this runaway takes place must contain sufficient nuclei, assumed to have been mixed into the accreted envelope, from an oxygen, neon, magnesium white dwarf. The amount of  $^{26}\text{Al}$  synthesized by novae with different heavy element abundances ( $Z$ ) is proportional to  $Z$ . The higher the value of  $Z$ , the larger the final mass fraction of  $^{26}\text{Al}$ .

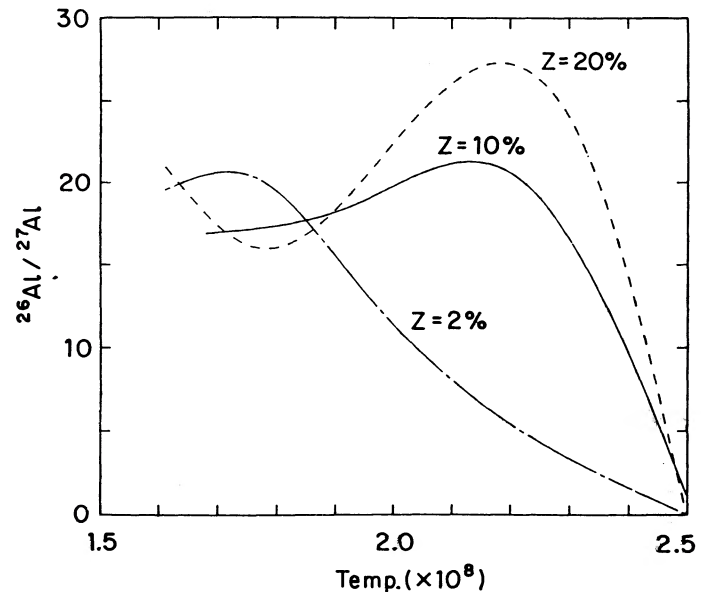


FIG. 9.—The effect of increasing the heavy element abundances on the ratio of  $^{26}\text{Al}/^{27}\text{Al}$ . The value of  $Z$  is the total mass fraction of C, N, O, Ne, Na, Mg, and Al. Their abundance ratios are obtained from a solar mixture (see text).

We also conclude that novae that reach a peak temperature of  $\sim 1.9 \times 10^8$  K for a period of time,  $\tau_{\text{ex}} \approx 100$  s, synthesize significant amounts of  $^{26}\text{Al}$ . However, if the peak temperature in the thermonuclear runaway is either higher than  $10^4$  s or much lower than 100 s, then that particular evolution will either consume  $^{26}\text{Al}$  or not synthesize it in any appreciable amounts.

We quantify this conclusion in the following way: Let the initial mass fraction of  $^{24}\text{Mg}$  and  $^{27}\text{Al}$  be  $\alpha \times ^{24}\text{Mg}_{\odot}$  and  $\beta \times ^{27}\text{Al}_{\odot}$ , respectively. We find from our calculations that the fraction of  $^{24}\text{Mg}_{\text{initial}}$  that is converted into  $^{26}\text{Al}$  is  $\approx 0.2$ .

Therefore, we predict

$$\text{Al}_{\text{Nova}}/\text{Al}_{\odot} = \beta + 0.2 \times \alpha \times \gamma$$

if the nova synthesizes  $^{26}\text{Al}$ , or

$$\text{Al}_{\text{Nova}}/\text{Al}_{\odot} = \beta + \text{small corrections}$$

if the nova does not reach the proper  $T_{\text{peak}}$  and  $\tau_{\text{ex}}$ . In this expression,  $\gamma$  is the ratio of  $^{24}\text{Mg}_{\odot}$  to  $^{27}\text{Al}_{\odot}$ .

Therefore, a nova that occurs on an ONeMg white dwarf, and which mixes core material into the accreted envelope, should show a ratio of  $\text{Al}_{\text{nova}}/\text{Al}_{\odot} \gg 100$  in the ejecta. If the nova does not show this high a ratio, then the peak conditions in the thermonuclear runaway were outside our most probable range of  $T_{\text{peak}}$  and  $\tau_{\text{ex}}$ .

A summary by Wiescher et al. (1986) of the observed compositions in novae gave, for Nova V693 CrA (1981), a value for the observed ratio of  $\text{Al}_{\text{nova}}/\text{Al}_{\odot} \approx 60$ . We conclude, therefore, that this nova did mix core material from an ONeMg white dwarf into the accreted envelope and then eject it into the ISM. We also note that the observed abundance enhancements in this nova (Williams et al. 1985) show that the white dwarf is losing mass as a result of the nova outburst.

It is interesting to estimate the total amount of  $^{26}\text{Al}$  produced in the Galaxy by the various types of nova. We classify observed novae into three subgroups: (a) Novae with solar abundances ( $\alpha, \beta = 1$ ); (b) Novae with high CNO or high O and Ne but with low Mg ( $1 \ll \alpha \ll 50$ ); (c) Novae with high O, Ne, and Mg ( $\alpha \gg 1, \beta \gg 1$ ).

The following additional information is required to determine the total amount of  $^{26}\text{Al}$  synthesized in the Galaxy. The number of novae of all kinds is about 40 nova galaxy $^{-1}$  yr $^{-1}$ . The fraction of ONeMg novae outbursts (high  $\alpha$  and  $\beta$ ) out of all observed novae outbursts is about 30% (Truran & Livio 1986). The mass ejected by novae is  $10^{-6}$  to  $10^{-7} M_{\odot}$  yr $^{-1}$  for class a and  $\sim 10^{-5} M_{\odot}$  yr $^{-1}$  for class b (Starrfield, Sparks, & Truran 1985). However, we do not know the fraction of novae in which the thermonuclear runaway on the white dwarf has evolved with the proper  $T_{\text{peak}}$  and  $\tau_{\text{ex}}$  for  $^{26}\text{Al}$  synthesis.

Using these numbers, we find that the maximum steady state amount of  $^{26}\text{Al}$  that can be maintained by the three classes is (a)  $10^{-3} M_{\odot}$  galaxy $^{-1}$  (if all the novae have solar abundances), (b)  $10^{-1} M_{\odot}$  galaxy $^{-1}$  (if 50% of all novae have  $1 \ll \alpha \ll 50$ ), and (c)  $5 M_{\odot}$  galaxy $^{-1}$  (if 30% of all nova are enriched in O, Ne, and Mg).

It should be stressed that these numbers are upper limits because they are obtained under the assumption that all novae evolve within the optimum range of  $T_{\text{peak}}$  and  $\tau_{\text{ex}}$ .

It is interesting to compare our results with those of Wiescher et al. (1986) since we used essentially the same nuclear reaction rates. First, note that the basic nova parameters used by Wiescher et al. (1986) were taken from older simulations where accretion onto the white dwarf was not included in the evolution. In the current study, we compared our results to simulations where accretion was included in the calculations and, therefore, the model parameters were different. Another basic difference can be traced to the assumed initial abundances of Ne, Na, and Mg. We have shown in this work that the amount of  $^{26}\text{Al}$  generated by a given nova is proportional to the amount of  $^{24}\text{Mg}$  at the beginning of the thermonuclear runaway and the abundance of  $^{24}\text{Mg}$  can become very high in an ONeMg white dwarf. Wiescher et al. (1986), however, assumed that  $^{24}\text{Mg}$  had a solar abundance. Hence, including these isotopes changes the results by large factors. Finally, we note that their studies were related more to C and O enriched novae and not the newly discovered (at that time) O, Ne, and Mg novae.

In summary, we note first that the observations (see Clayton & Leising 1987) imply that  $3 \pm 2 M_{\odot}$  of  $^{26}\text{Al}$  are produced in the Galaxy every  $10^6$  yr. Hence, if novae are the producers of  $^{26}\text{Al}$ , then the dominant contributors must be novae of class c. Second, if novae of class c are the dominant contributors of  $^{26}\text{Al}$ , then additional predictions can be made:

1. Novae that show Al enrichment should show also O, Ne, and Mg enrichments.
2. The predicted  $\text{Al}_{\text{nova}}/\text{Al}_{\odot}$  ratio for novae of class c should be greater than 100. This value is higher than that reported for V693 CrA 1981 (60; Williams et al. 1985). However, the abundance enhancements in this nova were still far from solar and it is easily possible that the Al abundance was at least a factor of 2 higher in the ejecta than reported by Williams et al. (1985). Nevertheless, based on the values that they reported we find that Nova V693 CrA (1981) was enriched in O and in Ne but not enough in Mg to make significant Al. On the other hand, Nova QU Vul (1984) showed much stronger Mg 2800 Å lines during its entire evolution (Saizar et al. 1990, in preparation) than did V693 CrA, and it is possible that the abundance analysis will show that it had a larger Mg abundance in its ejecta.

Of 12 recent well-observed novae (discussed by Truran & Livio 1986), four showed high O, Ne, and Mg. However, the amounts of Mg reported for these four novae may not have been enough to produce the required amounts of  $^{26}\text{Al}$ , although Al was strongly enhanced. Hence, it is probable that the estimate of 30% for those novae in the Galaxy that produce  $^{26}\text{Al}$  may be too optimistic.

We are grateful for a number of valuable discussions with M. Livio, J. Truran, and R. E. Williams. We are also grateful to the referee whose suggestions markedly improved the presentation. This work was supported in part by NSF grant AST88-18215 to Arizona State University, by the Institute of Geophysics and Planetary Physics at Los Alamos, by a NASA grant to Arizona State University (NAG5-481), and by the DOE.

#### REFERENCES

- Arnould, M., & Norgaard, H. 1978, A&A, 64, 195  
 Arnould, M., Norgaard, H., Thielemann F.-K., & Hillebrandt, W. 1980, ApJ, 237, 931  
 Ballmoos, P., Diehl, R., & Schonfelder, V. 1986, ApJ, 312, 134  
 Caughlan, G. R., Fowler, W. A., Harris, M. J., & Zimmermann, B. A. 1985, AtomDNDT, 32, 197

- Champagne, A. E., Howard, A. J., & Parker, P. D. 1983, *ApJ*, 269, 686  
 Chance, E. M., & Harris, M. J. 1979, *A&A*, 74, 247  
 Clayton, D. D. 1984, *ApJ*, 280, 144  
 Clayton, D. D., & Hoyle, F. 1974, *ApJ*, 187, L101  
 ——— 1976, *ApJ*, 203, 490  
 Clayton, D. D., & Leising, M. D. 1987, *PhyRp*, 144, 1  
 Fowler, W. A., Caughlan, G. R., & Zimmermann, B. A. 1975, *ARAA*, 13, 69  
 Harris, M. J., Fowler, W. A., Caughlan, G. R., & Zimmermann, B. A. 1983, *ARAA*, 21, 165  
 Hillebrandt, W., & Thielemann, F.-K. 1982, *ApJ*, 255, 617  
 Lee, T., Papanastassiou, D. A., & Wasserburg, G. J. 1977, *ApJ*, 211, L107  
 MacDonald, J. 1983, *ApJ*, 267, 732  
 Mahoney, W. A., Ling, J. C., Jacobson, A. S., & Lingenfelter, R. E. 1982, *ApJ*, 262, 742  
 Nomoto, K., Thielemann, F.-K., & Miyaji, S. 1985, *A&A*, 149, 239.  
 Prialnik, D., Livio, M., Shaviv, G., & Kovetz, A. 1982, *ApJ*, 257, 312  
 Share, G. H., Kinzer, R. L., Kurfess, J. D., Forrest, J. D., Chupp, F. L., & Rieger, E. 1985, *ApJ*, 292, L61  
 Starrfield, S. 1988, in *Multiwavelength Astrophysics*, ed. F. A. Cordova (Cambridge: Cambridge University Press), p. 159  
 Starrfield, S. 1989, in *The Classical Nova*, ed. N. Evans & M. Bode (New York: Wiley), p. 39  
 Starrfield, S., Sparks, W. M., & Shaviv, G. 1988, *ApJ*, 325, L35  
 Starrfield, S., Sparks, W. M., & Truran, J. W. 1985, *ApJ*, 291, 136.  
 ——— 1986, *ApJ*, 303, L5  
 Starrfield, S., Truran, J. W., & Sparks, W. M. 1978, *ApJ*, 226, 186  
 Truran, J. W., & Livio, M. 1986, *ApJ*, 308, 721  
 Urey, H. C. 1955, *Proc. Nat. Acad. Sci.*, 41, 127  
 Vangioni-Flam, E., Audouze, J., & Chieze, J.-P. 1980, *A&A*, 82, 234  
 Wagoner, R. V., Fowler, W. A., & Hoyle, F. 1967, *ApJ*, 148, 3  
 Wallace, R. K., & Woosley, S. E. 1981, *ApJS*, 45, 389  
 Ward, R. A., & Fowler, W. A. 1980, *ApJ*, 238, 266  
 Weaver, T. A., Zimmermann, G. B., & Woosley, S. E. 1978, *ApJ*, 225, 1021  
 Weber, W. R., Schonfelder, V., & Diehl, R. 1986, *Nature*, 323, 692  
 Wiescher, M., Gorres, J., Thielemann, F.-K., & Ritter, H. 1986, *A&A*, 160, 56  
 Wiescher, M., Harms, V., Gorres, J., Thielemann, F.-K., & Rybarczyk, L. J. 1987, *ApJ*, 316, 162  
 Williams, R. E., Sparks, W. M., Ney, E. P., Starrfield, S., & Truran, J. W. 1985, *MNRAS*, 212, 753  
 Woosley, S. E., and Weaver, T. A. 1980, *ApJ*, 238, 1017